Erschienen in: Macromolecular Materials and Engineering ; 303 (2018), 4. - 1700416
https://dx.doi.org/10.1002/mame.201700416

Thermoplastic Polyurethane Elastomers with Aliphatic Hard Segments Based on Plant-Oil-Derived Long-Chain Diisocyanates

*Brigitta Schemmer, Cathrin Kronenbitter, and Stefan Mecking**

Novel plant-oil-derived long-chain (C_{19} and C_{23}) α,ω-diisocyanates, optionally in combination with the corresponding long-chain diols, provide entirely aliphatic hard segments in segmented thermoplastic polyurethane elastomers (TPUs), with carbohydrate-based poly(trimethylene glycol) soft segments. Compared to materials based on a mid-chain monomer analog, phase separation is higher due to an increased flexibility of the aliphatic segments. Although melting points are slightly lower than for HDPE, the long-chain TPU's solid-state structure is still dominated by hydrogen-bonding.

1. Introduction

Segmented thermoplastic polyurethane elastomers (TPUs) are versatile materials that have found a wide variety of applications ranging from textile fibers, adhesives, foams, coatings, and biomaterials.[1] TPUs are linear multiblock copolymers composed of macrodiol soft segment blocks and urethane rich hard segment blocks. The incompatibility of hard and soft segment units results in phase separation with nanoscale hard segment domains dispersed in a continuous soft segment matrix.[2] Typical macrodiols serving as soft segments are relatively long, flexible polyester or polyether diols with a molecular weight of 1000–3000 g mol^{-1} like, for example, polycaprolactones and poly(tetramethylene glycol) which impart flexibility and ductility in TPUs. Hard segments that serve as load bearing phase are generally obtained by the reaction of diisocyanates with short diols, which produce polyurethane groups and include hydrogen bond formation between urethane groups thereby providing physical crosslinking. Commonly used monomers for hard segments are, for example, 1,4-butanediol as a short-chain diol and 4,4′-diphenylmethane diisocyanate (MDI) or toluene diisocyanate (TDI) as aromatic diisocyanate component.[3] In order to increase UV-light stability, thermal stability and optical clarity aromatic diisocyanates can be replaced by aliphatic diisocyanates, for example, isophorone diisocyanate (IPDI) and 1,6-hexane diisocyanate (HDI).[4,5] A class of aliphatic diisocyanates that has recently gained increasing interest are linear long-chain diisocyanates, which show potential for accessing a novel kind of TPUs combining the advantages of classical aliphatic TPUs with the possibility of exploiting polyethylene-like crystallinity. While linear diisocyanates containing up to 12 methylene units are commercially available, the synthesis of linear diisocyanates with longer methylene sequences up to eicosane diisocyanate[6a–d] has found less attention. While long-chain polyurethanes like PU-18,20 have been reported, thermoplastic elastomers with soft segments in combination with long-chain aliphatic crystalline segments are lacking.

To date, fatty acid derivatives are utilized for polyurethanes as polyol cross-linkers[5] and soft portions.[6e] However, α,ω-difunctional linear long-chain compounds have recently become available from common seed oils or algae oils[7] via biotechnological[8] or chemical catalytic routes such as metathesis[9] or isomerizing alkoxycarbonylation.[10] The long methylene sequences originating from complete incorporation of the entire fatty acid chain in these monomers provide access to novel long-chain monomers for long-chain aliphatic polycondensates.[11] We now report the synthesis of novel linear long-chain aliphatic diisocyanates based on oleic acid and erucic acid, and demonstrate their utility for the generation of all-aliphatic thermoplastic polyurethane elastomers.

B. Schemmer, C. Kronenbitter, Prof. S. Mecking
Chair of Chemical Materials Science
Department of Chemistry
University of Konstanz
Universitätsstrasse 10, D-78457 Konstanz, Germany
E-mail: stefan.mecking@uni-konstanz.de

2. Results and Discussion

2.1. Monomer Synthesis

Polyurethanes can be accessed by different routes, which have been reviewed comprehensively.[12] Especially transurethanization of dicarbamates has been studied as an isocyanate-free route. However, this method often results in low molecular weight polyurethanes.[12c] In order to avoid this issue in favor of material properties we utilized the high reactivity of isocyanates in this work. Unsaturated fatty acids were utilized as a source for the preparation of linear saturated dibromo compounds which were used as precursors for the synthesis of novel linear long-chain diisocyanates via a nucleophilic substitution reaction (**Figure 1**). In the first step isomering alkoxycarbonylation of methyl oleate (**1a**) and ethyl erucate (**1b**) yielded dimethyl nonadecanedioate (**2a**) and dimethyl tricosandioate (**2b**),[13] respectively, which were then reduced to obtain nonadecanediol

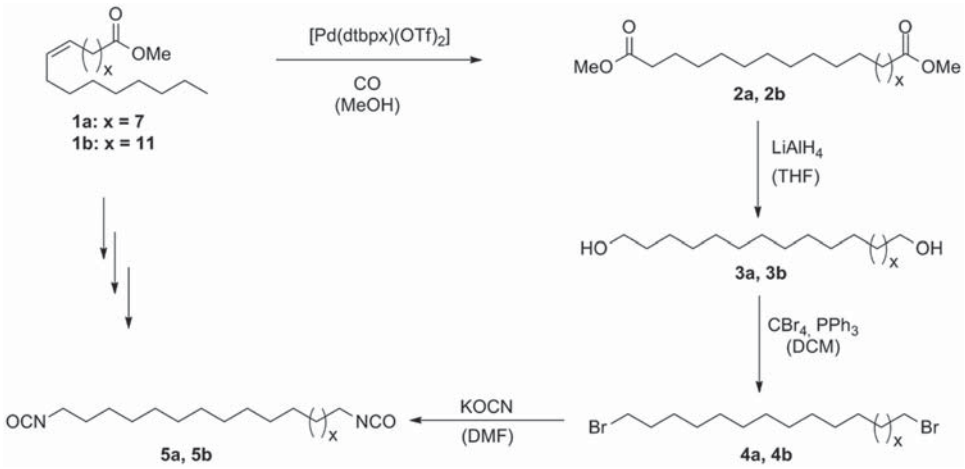

Figure 1. Synthesis of fatty acid based 1,19-diisocyanatononadecane and 1,23-diisocyanatotricosane.

(**3a**) and tricosanediol (**3b**).[14] In order to obtain the desired diisocyanates, the long-chain diols were converted into the corresponding dibromides (**4a, 4b**) via an Appel II reaction.[7] A subsequent nucleophilic substitution reaction with potassium cyanate based on a procedure reported by Schaeffer[15] yielded nonadecane diisocyanate (**5a**) and tricosane diisocyanate (**5b**) in yields up to 40% (Figure 1). Unlike rearrangement reactions which are frequently used for the synthesis of fatty acid based linear diisocyanates[6a,16] or dicarbamates,[17] this kind of nucleophilic substitution reaction does not result in shortening of the hydrocarbon chain. Optimization of reaction conditions and work up procedure yielded the desired diisocyanates in sufficient yields and in polycondensation grade purity. The structure of the synthesized diisocyanates was confirmed via NMR and Fourier transform infrared (FTIR) spectroscopy. The FTIR spectra showed strong characteristic bands at 2260 cm^{-1} corresponding to the N=CO stretching vibration (Figures S4 and S8, Supporting Information). ^{1}H and ^{13}C NMR spectra of the diisocyanates were in accordance with the proposed structures including a ^{13}C resonance at δ 122 ppm characteristic of isocyanate groups and confirmed purity higher than 98% (Figures S1–S3, S5–S7, Supporting Information).

2.2. Polymer Composition

In order to synthesize segmented thermoplastic polyurethane elastomers, the obtained fatty acid derived long-chain diisocyanates (**5a, b**) were copolymerized with the corresponding diols (**3a, b**) and a macrodiol in a one-step solvent polymerization procedure. Thereby, the long-chain diisocyanates (**5a, b**) and the corresponding diols (**3a, b**) provide entirely aliphatic hard segments. As a macrodiol for the generation of soft segments carbohydrate-based poly(trimethylene glycol) with a molecular weight of M_n = 2000 g mol^{-1} ($PPDO_{2000}$)[18] was employed. Copolymerization of these monomers yielded entirely aliphatic TPUs with molecular weights of M_n 3 to 5×10^4 g mol^{-1} according to end-group analysis from ^{1}H NMR spectroscopy. This is qualitatively confirmed by gel permeation chromatography (GPC) analysis which also shows well-behaved molecular weight distributions M_w/M_n around 1.7. As typical for TPUs based on aliphatic polyurethane hard segments, the obtained copolymers are transparent and become more opaque with increasing content of hard segment (**Figure 2** and Figure S9, Supporting Information). In order to further assess the effect of the long hydrocarbon chain of the aliphatic hard segments and compare these new hard segments with commercial hard segments, another polyurethane–polyether copolymer TPU-$C_{12}PPDO_{2000}$-59wt% (**Table 1**, entry 7) was prepared which is based on the commercial mid-chain aliphatic monomers 1,12-diisocyanatododecane and 1,12-dodecanediol and contains a weight fraction of polyether diol comparable to TPU-$C_{23}PPDO_{2000}$-63wt% (designation of the TPU materials list the monomer chain length of the hard block (e.g., C_{23}), the molecular weight of the PPDO soft block (e.g., 2000), and the relative weight portion of soft block (e.g., 63%, corresponding to 37 wt% hard block)). Apart from the fact that the shortest hard block, that is, an isolated diisocyanate repeat unit, is already twice as large for the long-chain monomer based polymer (C_{23}) compared to its mid-chain analog (C_{12}), their block length distributions and chain microstructure are similar.[19]

2.3. Thermal Properties

The DSC thermograms obtained for the synthesized long-chain TPUs feature two melting points, a low melting point in the range of –6 to 1 °C and a high melting point in the range of 62–116 °C (Table 1). These correspond to two domains formed by phase separation. The peak in the low temperature regime can be ascribed to soft segment melting while peaks in the

Figure 2. Optical appearance of injection molded test specimen of TPU-$C_{19}PPDO_{2000}$-85wt% and TPU-$C_{23}PPDO_{2000}$-83wt%.

Table 1. Molecular weights and thermal properties of polyurethane–polyether copolymers based on mid-chain and long-chain aliphatic hard segments.

Entry	Polymer	mol% $PPDO_{2000}$ of total diol	M_n[a] (NMR) [g mol^{-1}]	M_n[b] (GPC) [g mol^{-1}]	M_w/M_n[b]	T_m[c] [°C]	T_c[c] [°C]	T_g[d] [°C]
1	TPU-$C_{19}PPDO_{2000}$-85wt%	100%	3.1×10^4	5.1×10^4	1.5	–1/62	–18/32	–66
2	TPU-$C_{19}PPDO_{2000}$-78wt%	75%	3.2×10^4	4.5×10^4	1.7	–6/97	–23/68	–68
3	TPU-$C_{19}PPDO_{2000}$-67wt%	50%	2.9×10^4	4.2×10^4	1.6	–6/109	–31/78	–68
4	TPU-$C_{23}PPDO_{2000}$-83wt%	100%	5.0×10^4	5.7×10^4	1.7	1/76	–13/60	–68
5	TPU-$C_{23}PPDO_{2000}$-75wt%	75%	3.0×10^4	3.9×10^4	1.7	–4/102	–18/78	–69
6	TPU-$C_{23}PPDO_{2000}$-63wt%	50%	3.3×10^4	4.1×10^4	1.7	–6/116	–20/89	–69
7	TPU-$C_{12}PPDO_{2000}$-59wt%	29%	6.7×10^4	–	–	129	86	–66

[a]Determined by end-group analysis from ^{1}H NMR spectroscopy; [b]Determined by GPC in THF at 50 °C versus polystyrene standards; [c]Determined by DSC with a heating/cooling rate of 10 K min^{-1}; [d]Determined by DSC with a heating rate of 30 K min^{-1}.

higher temperature regime can be ascribed to the melting of the hard phase. Partial replacement of the polyether macromonomer by the long-chain aliphatic diol **3a** or **3b**, respectively, resulted in a significant increase of melt temperatures of the hard phase from 62 to 109 °C for C_{19}-TPUs and 76 to 116 °C for C_{23}-TPUs (**Figure 3**, Figures S13 and S14, Supporting Information).

This indicates more favorable crystallization conditions and an increased degree of ordering of the hard segment with increasing hard segment content. The same is true for replacing C_{19} long-chain monomers with corresponding C_{23} monomers, which results in increased melting temperatures of the hard phase and therefore higher melting points for C_{23}-TPUs. Comparison of long-chain TPU-$C_{23}PPDO_{2000}$-63wt% with the analogous mid-chain TPU-$C_{12}PPDO_{2000}$-59wt% showed an increase in the melting temperature by 13–129 °C which can be attributed to the higher content of urethane groups and the odd-even effect (Table 1, entry 7). If compared to analogous long-chain thermoplastic elastomers based on long-chain aliphatic polyester hard segments, the melting points of polyurethane–polyether copolymers are significantly enhanced due to hydrogen bonding between the urethane groups.[19]

Polycondensation of stoichiometric amounts of long-chain diisocyanate **5a** and **5b** with the corresponding long-chain diols **3a** and **3b** yielded PU-19,19 and PU-23,23, thermoplastic materials that showed melting points of 132 and 129 °C (Table S1, Figure S12, Supporting Information). As expected, the observed melting temperature decreases with increasing length of methylene sequences and therefore decreasing content of urethane groups due to reduced hydrogen bonding. Like for other long-chain polyurethanes[17,20] the melting temperatures are close to and even below that for linear polyethylene (T_m = 135 °C).[21] Considering the strong odd-even effects usually observed in the melting behavior of polyurethanes the melting points for PU-19,19 and PU-23,23 are surprisingly high.[22] Compared to PU-18,20 (T_m = 123 °C)[17] and PU-32,12 (T_m = 135 °C)[20]—polyurethanes with the same or almost the same content of urethane groups as PU-19,19 and PU-23,23, respectively—the melting points for PU-19,19 and PU-23,23 are in the same range and in case of PU-19,19 even higher than that for its even-even counterpart.

While PU-19,19 and PU-23,23 show no glass transition, all block copolymers studied show a glass transition point at ≈–68 °C due to the PPDO soft segment. Glass transition temperatures of the soft-segment phase of all synthesized TPUs essentially resemble the T_g observed for the neat soft segment oligomer $PPDO_{2000}$ (T_g = –70 °C), in agreement with a virtually complete phase separation for all TPUs studied.[23]

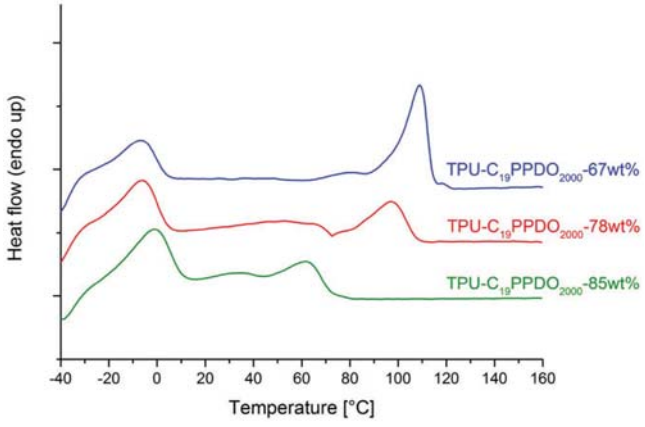

Figure 3. DSC thermograms (second heating) of polyurethane–polyether copolymers based on C_{19} monomers.

2.4. Mechanical Properties

Tensile tests were performed on specimens prepared by piston injection molding. All segmented polyurethane materials show ductile behavior typical for thermoplastic elastomers and exhibit an elongation at break higher than 250% which increases to 490% with increasing polyether content (typical stresses at break are 4–7 MPa). Segmented polyurethanes with hard segments based on C_{23} diisocyanate and diol instead of the corresponding C_{19} monomers generally exhibit a lower elongation at break except for TPUs with a very high hard segment content (**Table 2**, entry 3 and 6) which exhibit similar elongations at break within experimental error. As expected, Young's moduli decrease with increasing content of polyether soft segment for both polymer series ranging from 17 to 24 MPa for C_{19}-containing polyurethanes and 21 to 36 MPa for C_{23}-containing polyurethanes (Table 2, Figures S15 and S16, Supporting Information). This favorably places the investigated novel materials within the desirable range of 5–700 MPa reported for Young's moduli of commercial TPUs.[24] Comparison to the mid-chain analog TPU-$C_{12}PPDO_{2000}$-59wt% (Table 2, entry 7) showed that in materials with a similar portion of soft segment the choice of C_{23} versus C_{12} monomers had no significant effect on the Young's modulus with TPU-$C_{12}PPDO_{2000}$-59wt% exhibiting only a slightly higher Young's modulus of 39 MPa compared to TPU-$C_{23}PPDO_{2000}$-63wt% (E_m = 36 MPa), while the ductility improved drastically resulting in an increase of the elongation at break from 280 to 650%. This increase in ductility could not be explained with the

Table 2. Mechanical properties of polyurethane–polyether copolymers based on long-chain and mid-chain aliphatic hard segments.

Entry	Polymer	Young's mod.[a,b] [MPa]	Elongation at break[a,c] [%]	Residual strain[d] [%]
1	TPU-C_{19}PPDO$_{2000}$-85wt%	17 ± 3	470 ± 52	26
2	TPU-C_{19}PPDO$_{2000}$-78wt%	22 ± 2	450 ± 49	33
3	TPU-C_{19}PPDO$_{2000}$-67wt%	24 ± 2	270 ± 70	31
4	TPU-C_{23}PPDO$_{2000}$-83wt%	22 ± 2	440 ± 29	32
5	TPU-C_{23}PPDO$_{2000}$-75wt%	21 ± 4	270 ± 85	39
6	TPU-C_{23}PPDO$_{2000}$-63wt%	36 ± 2	280 ± 32	37
7	TPU-C_{12}PPDO$_{2000}$-59wt%	39 ± 1	650 ± 13	29

[a]Tensile tests according to ISO 527/1-2, specimen type 5A prepared by injection molding; [b]Crosshead speed 1 mm min^{-1}; [c]Crosshead speed 500 mm min^{-1}; [d]Determined from hysteresis experiments after ten cycles at an elongation of 100% with a crosshead speed of 50 mm min^{-1}.

odd-even effect but has to be attributed to increased hydrogen bond formation due to a higher urethane content.[25]

In order to assess the elastic properties of the polyurethane–polyether copolymers cyclic hysteresis tests were performed. Test specimens were repeatedly exposed to consecutive cycles of loading to a constant strain of 100% and unloading. After the first few cycles, where hysteresis is observed and the residual deformation gradually increases, all TPUs exhibit a virtually constant level of recovery. This behavior is typical of thermoplastic elastomers[2,26] and can be ascribed to the adoption of a largely constant structure after an initial change in morphology with alignment of the polymer microstructure.[27] For the segmented polyurethane–polyether copolymers studied here elastomeric behavior is observed for all polymers and residual strains after ten cycles range between 26 and 33% (Table 2, **Figure 4**) for C_{19} copolymers and between 32 and 39% (Table 2, Figure S17, Supporting Information) for C_{23} copolymers. For

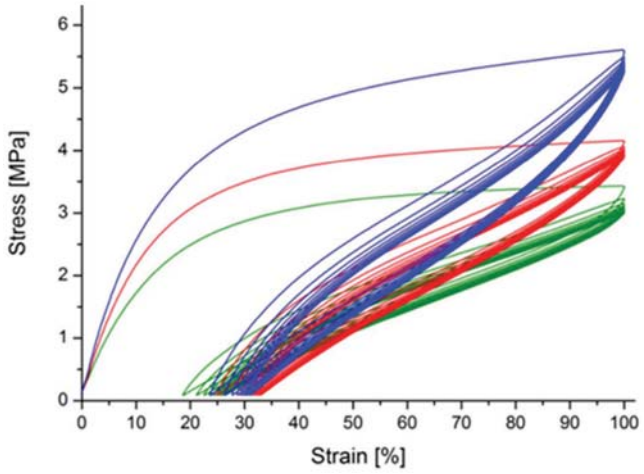

Figure 4. Stress–strain curves from cyclic tensile tests with a constant strain of 100% for polyurethane–polyether copolymers TPU-C_{19}PPDO$_{2000}$-67wt% (blue), TPU-C_{19}PPDO$_{2000}$-78wt% (red), and TPU-C_{19}PPDO$_{2000}$-85wt% (green) (10 cycles).

both polymer series the observed residual strain differs only slightly with varying content of hard and soft segment, though the highest level of recovery is observed for polymers without a long-chain diol as an additional component contributing to the crystalline phase. Comparison of TPU-C_{23}PPDO$_{2000}$-63wt% with the mid-chain analog TPU-C_{12}PPDO$_{2000}$-59wt% showed that C_{12} versus C_{23} monomers results in improved elastic behavior with a decrease of residual strain from 37 to 29% (Figure S18 and Table 2, entry 6 and 7), indicating that longer methylene sequences and therefore a lower content of urethane groups resulted in a decrease of elasticity.

2.5. FTIR Spectroscopy

Attenuated total reflection Fourier transform infrared (ATR-FTIR) spectroscopy was used to investigate the composition of the synthesized polyurethanes and determine the relative degree of phase separation. The FTIR spectra show distinct bands related to amide and carbonyl groups at 3334, 1723, and 1683 cm^{-1}, respectively. The lack of an isocyanate peak at 2260 cm^{-1} and the presence of the amide and carbonyl peaks confirm complete conversion of the monomers to urethane (Figures S19 and S20, Supporting Information).

As the degree of phase separation directly influences the mechanical properties of thermoplastic elastomers, FTIR spectroscopy was used to investigate the microphase morphology and gain further insight into the relation between polymer composition and mechanical properties. Urethane amide groups can form hydrogen bonds with urethane carbonyl groups of hard segments resulting in the formation of hard segment domains as well as with ether groups of soft segments resulting in phase mixing. Therefore, the extent of hydrogen bonding between the urethane amide and carbonyl groups was investigated by FTIR spectroscopy to determine the degree of phase separation.

The shift of the amide band to 3334 cm^{-1} and the absence of further amide bands at about 3400 cm^{-1} suggests the presence of only hydrogen bonded amide hydrogens. Closer analysis of the carbonyl region shows the presence of two carbonyl signals at 1723 and 1683 cm^{-1} (**Figure 5** and Figure S21, Supporting Information). Carbonyls that are organized and strongly hydrogen bonded to amides possess restricted vibrational motions resulting in a lower absorption frequency and the observed peak at 1683 cm^{-1} in the FTIR spectra compares well with a reported value of 1685 cm^{-1} for strongly hydrogen bonded carbonyl groups.[28] Additional IR bands of carbonyls not involved in hydrogen bonding would be expected at about 1730 cm^{-1}, while carbonyl associated with poorly ordered hydrogen bonding are to be expected at about 1710 cm^{-1}.[3a,28] Accordingly the carbonyl band at 1723 cm^{-1} can be assigned to non-hydrogen bonded carbonyl groups. The deviation from literature values can be attributed to differences in the structure of the hard segment components. With increasing content of hard segment the carbonyl band at 1683 cm^{-1} starts to broaden and peak deconvolution suggests the presence of an additional overlapping signal at about 1702 cm^{-1} associated with poorly ordered hydrogen bonding. This indicates the formation of larger hard segment domains with imperfect hydrogen bonding

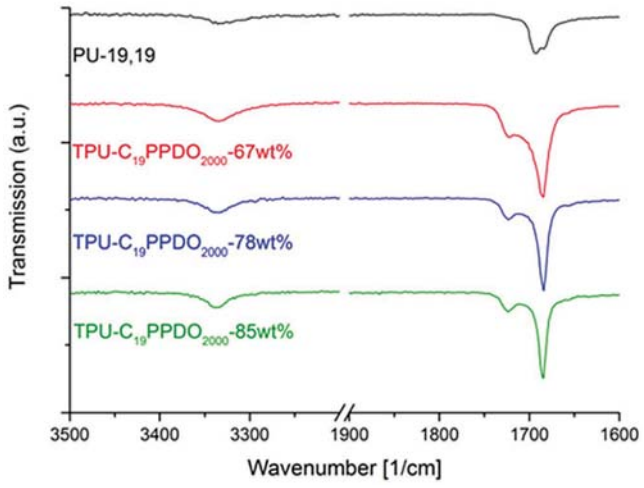

Figure 5. Amide and carbonyl regions of the FTIR spectra of polyurethanes based on C_{19} monomers.

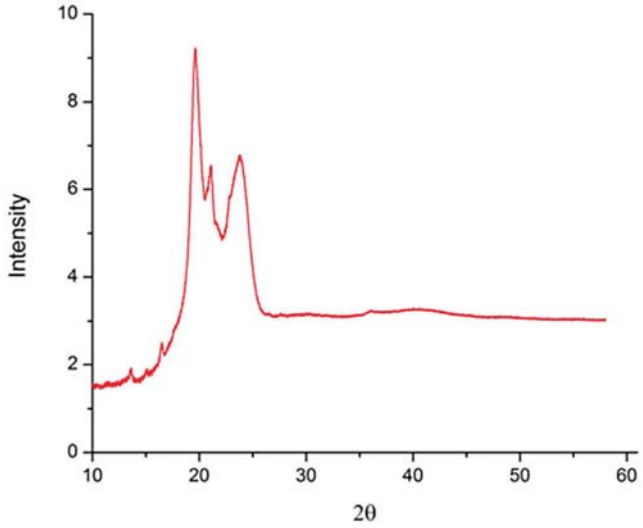

Figure 6. WAXD pattern of PU-19,19.

especially for TPU-C_{19}PPDO$_{2000}$-67wt% and TPU-C_{23}PPDO$_{2000}$-63wt%. For PU-19,19 and PU-23,23 broad peaks at 1693 and 1685 cm^{-1} are observed suggesting overlapping of multiple signals (Figure 5 and Figure S21, Supporting Information).

In order to obtain a quantitative measure of the relative amounts of different carbonyl groups present and to determine the extent of phase separation, the carbonyl regime of the FTIR spectra was analyzed by peak deconvolution of the carbonyl absorption bands. The percentage of each carbonyl signal was obtained by comparing the specific peak areas with the total peak area (**Table 3**). The results indicate the presence of about 15% of free carbonyl groups for all long-chain TPUs implying a high degree of phase separation of about 85% regardless of the polymer composition which is only achieved by annealing for other TPUs based on aromatic or cycloaliphatic hard segments.[28b,29] In comparison, IR analysis of TPU-C_{12}PPDO$_{2000}$-59wt% based on mid-chain C12 monomers showed a much lower degree of phase separation of 56% (Figure S22, Supporting Information, and Table 3, entry 7) indicating that increased chain flexibility due to longer methylene sequences promotes hydrogen bond formation and phase separation.

Table 3. Quantitative analysis of the carbonyl region of FTIR spectra for TPUs by peak deconvolution.

Entry	Polymer	Peak area [%]	
		Free C=O groups (1723 cm^{-1})	H-bonded C=O groups (1702 cm^{-1} + 1685 cm^{-1})
1	TPU-C_{19}PPDO$_{2000}$-85wt%	13	87
2	TPU-C_{19}PPDO$_{2000}$-78wt%	13	87
3	TPU-C_{19}PPDO$_{2000}$-67wt%	14	86
4	TPU-C_{23}PPDO$_{2000}$-83wt%	15	85
5	TPU-C_{23}PPDO$_{2000}$-75wt%	15	85
6	TPU-C_{23}PPDO$_{2000}$-63wt%	13	87
7	TPU-C_{12}PPDO$_{2000}$-59wt%	54[a)]	56[b)]

[a)]Signal at 1720 cm^{-1}; [b)]Signal at 1680 cm^{-1}.

2.6. X-Ray Diffraction

The crystalline solid state structures of the studied novel long-chain polyurethanes were elucidated by WAXS. While long-chain polyesters crystallize in the polyethylene-like orthorhombic structure with ester groups being incorporated in the all-trans hydrocarbon crystal lattice as defects[29] crystalline structures of polyurethanes are dominated by intermolecular hydrogen bonds between urethane groups.[30] The WAXS diffraction patterns of PU-19,19 and PU-23,23 as well as corresponding TPUs displayed peaks at 2θ angles of 19.6°, 21.1°, and 23.6° corresponding to *d*-spacings of 4.5, 4.2, and 3.8 Å (**Figure 6** and Figure S23, Supporting Information). These values do not concur with orthorhombic polyethylene WAXS diffraction peaks at *d*-spacings of 4.1 Å (d_{110}) and 3.7 Å (d_{200}).[31] In this sense, the long-chain TPUs do not possess a polyethylene-like structure. Rather the *d*-spacings of the two prominent diffraction peaks at 19.6° and 23.6° appear to be related to the characteristic two reflection peaks (4.4 Å (d_{100}) and 3.7 Å (d_{010})) typically seen for even-even polyamides or polyurethanes in a triclinic crystal phase.[32] The weaker diffraction peak at 21.1° (4.2 Å) corresponds to a pseudohexagonal phase indicating an overall crystal structure composed of triclinic and pseudohexagonal cells. These results correspond to the crystal structures reported for aliphatic polyurethanes based on short-chain diisocyanates and long-chain diols.[30b] Therefore, despite the long methylene sequences, hydrogen bonding is still a dominating factor in the crystallization processes of polyurethanes based on C_{19} and C_{23} monomers, resulting in similar crystal structure as for polyurethanes with higher hydrogen-bonding densities.

3. Experimental Section

3.1. Materials and General Considerations

Methylene chloride was distilled from CaH_2. DMF and 1,1,2,2-tetrachloroethane were dried over molecular sieves (3 Å).

n-Heptane (Emplura 99%) was purchased from Merck and methanol (99.8%) from Sigma-Aldrich. All other solvents were used in technical grade as received. Tetrabromomethane (98%) was purchased from ABCR, triphenylphosphine (99%) from Acros Organics, potassium cyanate (96%) from Sigma Aldrich, and *N*,*N*′-di-2-naphthyl-1,4-phenylenediamine (>96%) from TCI Europe. Poly(trimethylene glycol) with a number average molecular mass of M_n = 2000 kindly donated by Allessa GmbH was degassed prior to use. Dimethyl-1,23-tricosanedioate[13] and tricosane-1,23-diol[14] as well as dimethyl-1,19-nonadecanedioate,[13] and nonadecane-1,19-diol[14] were prepared from methyl erucate and methyl oleate, respectively, according to previously reported literature procedures. All reactions were carried out under standard Schlenk conditions under a nitrogen atmosphere.

3.2. Characterization

NMR spectra were recorded on a Varian Inova 400 and a Bruker Avance 400 spectrometer. ^{1}H and ^{13}C chemical shifts were referenced to the solvent signals. DSC analyses were performed on a Netzsch Phoenix 204 F1 instrument with a heating and cooling rate, respectively, of 10 K min^{-1} in a temperature range of –50 to 160 °C. Data reported are from second heating cycles. GPC measurements were carried out on a Polymer Laboratories PL-GPC 50 with two PLgel 5 µm MIXED-C columns in THF at 50 °C against polystyrene standards with refractive index detection or on a Polymer Laboratories 220 instrument equipped with Olexis columns with differential refractive index, viscosity, and light-scattering (15° and 90°) detectors in 1,2,4-trichlorobenzene at 160 °C against linear polyethylene standards. Tensile testing was performed on dogbone-shaped sample bars (75 × 12.5 × 2 mm^3; ISO 527-2, type 5A) which were prepared using a HAAKE Minijet II (Thermo Scientific) piston injection molder. 0.1 wt% of *N*,*N*′-di-2-naphthyl-1,4-phenylenediamine were employed as a stabilizer. After preconditioning the samples overnight tensile tests were performed on a Zwick 1446 Retroline tC II instrument according to ISO 527 (crosshead speed 500 mm min^{-1}, with a determination of the Young's modulus at a crosshead speed of 1 mm min^{-1}). The Zwick test Xpert software version 11.0 was used to collect and analyze the data. Young's modulus, yield stress, yield strain, tensile stress at break, and tensile strain at break were obtained by averaging the data from several test specimens. Cyclic hysteresis tests were performed on dogbone-shaped sample bars (75 × 12.5 × 2 mm^3; ISO 527-2, type 5A) . The test specimens were repeatedly exposed to consecutive cycles of loading and unloading to a constant strain of 100% with a constant crosshead speed of 50 mm min^{-1}. The recovery was measured by observing the residual strain after ten cycles. ATR-FTIR spectra were redorded on a PerkinElmer Spectrum100 FTIR Spectrometer equipped with a Universal ATR Sampling Accessory. FTIR scans were collected on injection molded dogbone-shaped sample bars (75 × 12.5 × 2 mm^3; ISO 527-2, type 5A). The frequency range covered was from 4000 to 650 cm^{-1} by averaging 32 scans at a resolution of 2 cm^{-1}. Wide angle X-ray diffraction (WAXD) was performed on a Bruker AXS D8 Advance diffractometer using CuKα1 radiation. Diffraction patterns were recorded in the range 10°–60° 2θ, at 25 °C. Polymer samples for WAXD were prepared by crystallization from hot tetrachloroethane.

3.3. Monomer Synthesis

3.3.1. 1,19-Dibromononadecane

1,19-Nonadecanediol (11.4 g, 37.9 mmol) and CBr_4 (31.4 g, 94.8 mmol) were suspended in 500 mL methylene chloride and triphenylphosphine (26.9 g, 102.4 mmol) was slowly added as a solid over 30 min. The yellow solution was then heated to 50 °C for 1 h and afterward stirred at room temperature overnight. Then 100 mL methanol and 10 mL water were added and the solution stirred for 10 min at room temperature. The solvent was removed to obtain a beige solid, which was dissolved in 200 mL *n*-pentane and methanol. After extraction with pentane (3 × 200 mL) the combined pentane phases were washed once with 200 mL of water and the solvent then removed. Column chromatography with methylene chloride and subsequent crystallization from ethanol/ethylacetat (4:1) yielded 14.5 g of a white solid (34.0 mmol, 88%).[7]

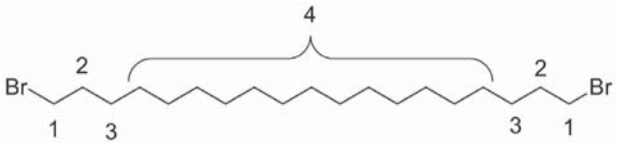

^{1}H NMR ($CDCl_3$, 25 °C, 400 MHz) δ 3.41 (t, $^3J_{H–H}$ = 7.0 Hz, 4H, H-1), 1.85 (qint, $^3J_{H–H}$ = 7.0 Hz, 4H, H-2), 1.42 (quint, $^3J_{H–H}$ = 7.0 Hz, 4H, H-3), 1.35–1.21 (m, 26H, H-4). ^{13}C NMR (101 MHz, $CDCl_3$) δ 34.2 (C-1), 33.0 (C-2), 29.8–29.6 (C-4), 28.9 (C-4), 28.3 (C-3).

3.3.2. 1,23-Dibromotricosane

1,23-Dibromotricosane was prepared analogous to the aforementioned procedure. The desired product was isolated as a white solid in 90% yield.[7]

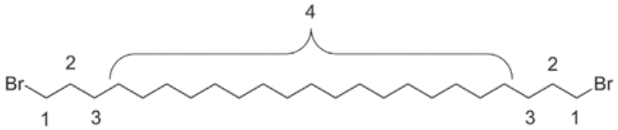

^{1}H NMR ($CDCl_3$, 25 °C, 400 MHz) δ 3.41 (t, $^3J_{H–H}$ = 7.0 Hz, 4H, H-1), 1.85 (qint, $^3J_{H–H}$ = 7.0 Hz, 4H, H-2), 1.42 (quint, $^3J_{H–H}$ = 7.0 Hz, 4H, H-3), 1.35–1.21 (m, 34H, H-4). ^{13}C NMR (101 MHz, $CDCl_3$) δ 34.2 (C-1), 33.0 (C-2), 29.8–29.6 (C-4), 28.9 (C-4), 28.3 (C-3).

3.3.3. 1,19-Diisocyanatononadecane

1,19-Dibromononadecane (3.0 g, 7.0 mmol) was dissolved in 50 mL DMF and the solution heated to 120 °C. Potassium cyanate (2.9 g, 35.2 mmol) was added and the suspension stirred at 120 °C for 35 min. Then the reaction mixture was

extracted with *n*-heptane (3 × 100 mL) and the combined *n*-heptane phases washed with water. After drying over $MgSO_4$, filtration and removing of the solvent the crude product was distilled using a sublimation apparatus with a cold finger (130 °C, 0.06 mbar) to give 860 mg of a white solid (2.5 mmol, 35%).

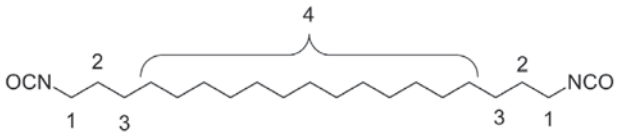

^{1}H NMR ($CDCl_3$, 25 °C, 400 MHz) δ 3.29 (t, $^3J_{H-H}$ = 6.7 Hz, 4H, H-1), 1.61 (quint, $^3J_{H-H}$ = 6.7 Hz, 4H, H-2), 1.41–1.33 (m, 4H, H-3), 1.33–1.21 (m, 26H, H-4). ^{13}C NMR (101 MHz, $CDCl_3$) δ 122.0 (NCO), 43.1 (C-1), 31.4 (C-2), 29.8–29.5 (C-4), 29.1 (C-4), 26.7 (C-3).

3.3.4. 1,23-Diisocyanatotricosane

1,23-Diisocyanatotricosane was prepared analogous to the aforementioned procedure. The desired product was isolated by distillation (140 °C, 0.06 mbar) to give a white solid in 40% yield.

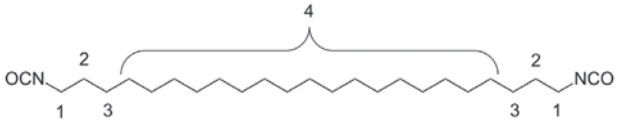

^{1}H NMR ($CDCl_3$, 25 °C, 400 MHz) δ 3.29 (t, $^3J_{H-H}$ = 6.7 Hz, 4H, H-1), 1.61 (quint, $^3J_{H-H}$ = 6.7 Hz, 4H, H-2), 1.42–1.33 (m, 4H, H-3), 1.33–1.21 (m, 34H, H-4). ^{13}C NMR (101 MHz, $CDCl_3$) δ 122.1 (NCO), 43.1 (C-1), 31.4 (C-2), 29.8–29.6 (C-4), 29.1 (C-4), 26.7 (C-3).

3.3.5. General Polymerization Procedure

After weighing in the desired amount of freshly distilled long-chain diisocyanate, long-chain diol (optional), and $PPDO_{2000}$ the mixture was degassed and dissolved in 20 mL of DMF (for TPU-$C_{19}PPDO_{2000}$-85wt%) or 1,1,2,2-tetrachloroethane (for all other polyurethanes). Then 0.5 mol% of dibutyltin dilaurate was added and the solution heated to 80 °C and stirred for 24 h. The reaction was stopped by adding 5 mL of methanol and after stirring for another 15 min the polymer was precipitated by pouring the reaction mixture into methanol. After filtration the white rubber-like polymer was dried in vacuo at 50 °C for 48 h.

4. Conclusions

In summary, two novel linear long-chain diisocyanates 1,19-diisocyanatononadecane and 1,23-diisocyanatotricosane were successfully synthesized from oleic acid and erucic acid esters via nucleophilic substitution. Polyaddition of these bio-based long-chain diisocyanates and their corresponding long-chain diols with diol-terminated $PPDO_{2000}$ yielded entirely bio-based transparent polyurethane–polyether copolymers with molecular weights up to M_n 5.0 × 10^4 g mol^{-1}. The long-chain aliphatic polyurethane segments provide physical crosslinking via hydrogen bonding resulting in melting points up to 116 °C and elastomeric behavior of these thermoplastic materials. A particularly high recovery was observed if no additional long-chain diol was incorporated. FTIR spectroscopy showed well-separated microphase morphologies and strongly hydrogen-bonded hard segments. Comparison to an analogous mid-chain monomer based polyurethane–polyether copolymer showed that applying long-chain monomers and the resulting lower content of urethane groups in the copolymer resulted in lower melting points and decreased ductility and elasticity but promoted phase separation.

Acknowledgements

B.S. is grateful for a stipend provided by the State of Baden-Württemberg through the Landesgraduiertenförderungsgesetz.

Conflict of Interest

The authors declare no conflict of interest.

Keywords

catalysis, fatty acid, polyurethane, renewable ressource, thermoplastic elastomer

[1] a) G. Woods, *The ICI Polyurethanes Book*, Wiley, New York **1990**; b) M. D. Lelah, S. L. Cooper, *Polyurethanes in Medicine*, CRC Press, Boca Raton, FL **1986**; c) *Block Polymers* (Ed: S. L. Aggarwal), Plenum, New York **1970**.

[2] G. Holden, H. R. Kricheldorf, R. P. Quirk, *Thermoplastic Elastomers*, Hanser, Munich, Germany **2004**.

[3] a) Z. S. Petrovic, J. Ferguson, *Prog. Polym. Sci.* **1991**, *16*, 695; b) P. Król, *Prog. Mater Sci.* **2007**, *52*, 915; c) Y. He, D. Xie, X. Zhang, *J. Mater. Sci.* **2014**, *49*, 7339.

[4] D. K. Chattopadhyay, D. C. Webster, *Prog. Polym. Sci.* **2009**, *34*, 1068.

[5] a) D. Randall, S. Lee, *The Polyurethanes Book*, Wiley, New York **2002**; b) C. Hepburn, *Polyurethane Elastomers*, Springer, Berlin **2012**.

[6] a) L. Hojabri, X. Kong, S. S. Narine, *J. Polym. Sci., Part A: Polym. Chem.* **2010**, *48*, 3302; b) E. Perry, J. Savory, *J. Appl. Polym. Sci.* **1967**, *11*, 2473; c) Y. Iwakura, K. Uno, K. Suzuki, K. Fujii, *Nippon Kageku Zasshi* **1957**, *78*, 1507; d) Y. Iwakura, K. Uno, K. Suzuki, K. Fujii, *Nippon Kageku Zasshi* **1957**, *78*, 1511. e) S. Schmidt, F. J. Gatti, M. Luitz, B. S. Ritter, B. Bruchmann, R. Mülhaupt, *Macromolecules* **2017**, *50*, 2296.

[7] P. Roesle, F. Stempfle, S. K. Hess, J. Zimmerer, C. Río Bártulos, B. Lepetit, A. Eckert, P. G. Kroth, S. Mecking, *Angew. Chem., Int. Ed.* **2014**, *53*, 6800.
[8] a) U. Schörken, P. Kempers, *Eur. J. Lipid Sci. Technol.* **2009**, *111*, 627; b) S. Schaffer, T. Haas, *Org. Process Res. Dev.* **2014**, *18*, 752; c) W. Lu, J. E. Ness, W. Xie, X. Zhan, J. Minshull, R. A. Gross, *J. Am. Chem. Soc.* **2010**, *132*, 15451.
[9] a) M. B. Dinger, J. C. Mol, *Adv. Synth. Catal.* **2002**, *344*, 671; b) H. Ngo, K. Jones, T. Foglia, *J. Am. Oil Chem. Soc.* **2006**, *83*, 629.
[10] a) C. Jiménez-Rodriguez, G. R. Eastham, D. J. Cole-Hamilton, *Inorg. Chem. Commun.* **2005**, *8*, 878; b) P. Roesle, C. J. Dürr, H. M. Möller, L. Cavallo, L. Caporaso, S. Mecking, *J. Am. Chem. Soc.* **2012**, *134*, 17696.
[11] F. Stempfle, P. Orgmann, S. Mecking, *Chem. Rev.* **2016**, *116*, 4597.
[12] a) O. Kreye, H. Mutlu, M. A. R. Meier, *Green Chem.* **2013**, *15*, 1431; b) L. Maisonneuve, T. Lebarbé, E. Grau, H. Cramail, *Polym. Chem.* **2013**, *4*, 5472; c) L. Maisonneuve, O. Lamarzelle, E. Rix, E. Grau, H. Cramail, *Chem. Rev.* **2015**, *115*, 12407.
[13] F. Stempfle, B. S. Ritter, R. Mülhaupt, S. Mecking, *Green Chem.* **2014**, *16*, 2008.
[14] D. Quinzler, S. Mecking, *Angew. Chem., Int. Ed.* **2010**, *49*, 4306.
[15] W. D. Schaeffer, (Union Oil Company of California), *US 3017420*, **1962**.
[16] a) A. S. More, T. Lebarbé, L. Maisonneuve, B. Gadenne, C. Alfos, H. Cramail, *Eur. Polym. J.* **2013**, *49*, 823; b) C. Fu, Z. Zheng, Z. Yang, Y. Chen, L. Shen, *Prog. Org. Coat.* **2013**, *77*, 53.
[17] M. Unverferth, O. Kreye, A. Prohammer, M. A. R. Meier, *Macromol. Rapid Commun.* **2013**, *34*, 1569.
[18] a) Press release by DuPont, Tate & Lyle of June 8, **2007**; b) M. A. Harmer, D. C. Confer, C. K. Hoffman, S. C. Jackson, A. Y. Liauw, A. R. Minter, E. R. Murphy, R. E. Spence, H. B. Sunkara, *Green Chem.* **2010**, *12*, 1410.
[19] F. Stempfle, B. Schemmer, A.-L. Oechsle, S. Mecking, *Polym. Chem.* **2015**, *6*, 7133.
[20] R. L. McKiernan, S. P. Gido, J. Penelle, *Polymer* **2002**, *43*, 3007.
[21] J. E. O'Gara, K. B. Wagener, S. F. Hahn, *Makromol. Chem., Rapid Commun.* **1993**, *14*, 657.
[22] a) R. M. Versteegen, R. P. Sijbesma, E. W. Meijer, *Angew. Chem., Int. Ed.* **1999**, *38*, 2917; b) S. Neffgen, J. Kušan, T. Fey, H. Keul, H. Höcker, *Macromol. Chem. Phys.* **2000**, *201*, 2108.
[23] Y. Camberlin, J. P. J. Pascualt, *J. Polym. Sci., Polym. Chem. Ed.* **1983**, *21*, 415.
[24] T. Ouhadi, S. Abdou-Sabet, H.-G. Wussow, L. M. Ryan, L. Plummer, F. E. Baumann, J. Lohmar, H. F. Vermeire, F. L. G. Malet, in *Ullmann's Encyclopedia of Industrial Chemistry* (Eds: W. Gerhartz, B. Elvers), Wiley-VCH, Weinheim **2014**, p. 1.
[25] L. Hojabri, X. Kong, S. Narine, *Biomacromolecules* **2009**, *10*, 884.
[26] A. Schmidt, W. S. Veeman, V. M. Litvinov, W. Gabriëlse, *Macromolecules* **1998**, *31*, 1652.
[27] a) M. A. Hood, B. Wang, J. M. Sands, J. J. La Scala, F. L. Beyer, C. Y. Li, *Polymer* **2010**, *51*, 2191; b) I. Yilgor, E. Yilgor, I. G. Guler, T. C. Ward, G. L. Wilkes, *Polymer* **2006**, *47*, 4105.
[28] a) R. Hernandez, J. Weksler, A. Padsalgikar, T. Choi, E. Angelo, J. S. Lin, L.-C. Xu, C. A. Siedlecki, J. Runt, *Macromolecules* **2008**, *41*, 9767; b) I. Yilgor, E. Yilgor, G. L. Wilkes, *Polymer* **2015**, *58*, A1.
[29] a) P. Ortmann, S. Mecking, *Macromolecules* **2013**, *46*, 7213; b) J. Trzaskowski, D. Quinzler, C. Bährle, S. Mecking, *Macromol. Rapid Commun.* **2011**, *32*, 1352; c) C. Le Fevere De Ten Hove, J. Penelle, D. A. Ivanov, A. M. Jonas, *Nat. Mater.* **2004**, *3*, 33.
[30] a) Y. Saito, K. Hara, S. Kinoshita, *Polym. J.* **1982**, *14*, 19; b) R. L. McKiernan, A. M. Heintz, S. L. Hsu, E. D. T. Atkins, J. Penelle, S. P. Gido, *Macromolecules* **2002**, *35*, 6970; c) A. M. Heintz, R. L. McKiernan, S. P. Gido, J. Penelle, S. L. Hsu, S. Sasaki, A. Takahara, T. Kajiyama, *Macromolecules* **2002**, *35*, 3117; d) R. L. McKiernan, P. Sikorski, E. D. T. Atkins, S. P. Gido, J. Penelle, *Macromolecules* **2002**, *35*, 8433.
[31] C. W. Bunn, *Trans. Faraday Soc.* **1939**, *35*, 482.
[32] C. W. Bunn, E. V. Garner, *Proc. R. Soc. London, Part A* **1947**, *189*, 39.